inorganics

MDPI

Review

Exploring Metal- and Porphyrin-Modified TiO_2-Based Photocatalysts for Efficient and Sustainable Hydrogen Production

Dimitrios Rafail Bitsos [1], Apostolos Salepis [1], Emmanouil Orfanos [1], Athanassios G. Coutsolelos [2,3], Ramonna I. Kosheleva [1], Athanassios C. Mitropoulos [1] and Kalliopi Ladomenou [1,*]

[1] Hephaestus Laboratory, School of Chemistry, Faculty of Science, Democritus University of Thrace, Kavala University Campus, St. Lucas, 65404 Kavala, Greece; dibitso@chem.duth.gr (D.R.B.); amitrop@chem.duth.gr (A.C.M.)
[2] Laboratory of Bioinorganic Chemistry, Chemistry Department, University of Crete, 70013 Heraklion, Greece; acoutsol@uoc.gr
[3] Foundation for Research and Technology (FORTH), Institute of Electronic Structure and Laser (IESL), 70013 Heraklion, Greece
* Correspondence: kladomenou@chem.duth.gr

Abstract: Photocatalytic H_2 production is one of the most promising approaches for sustainable energy. The literature presents a plethora of carefully designed systems aimed at harnessing solar energy and converting it into chemical energy. However, the main drawback of the reported photocatalysts is their stability. Thus, the development of a cost-effective and stable photocatalyst, suitable for real-world applications remains a challenge. An ideal photocatalyst for H_2 production must possess appropriate band-edge energy positions, an effective sacrificial agent, and a suitable cocatalyst. Among the various photocatalysts studied, TiO_2 stands out due to its stability, abundance, and non-toxicity. However, its efficiency in the visible spectrum is limited by its wide bandgap. Metal doping is an effective strategy to enhance electron–hole separation and improve light absorption efficiency, thereby boosting H_2 synthesis. Common metal cocatalysts used as TiO_2 dopants include platinum (Pt), gold (Au), copper (Cu), nickel (Ni), cobalt (Co), ruthenium (Ru), iron (Fe), and silver (Ag), as well as bimetallic combinations such as Ni-Fe, Ni-Cu, Nb-Ta, and Ni-Pt. In all cases, doped TiO_2 exhibits higher H_2 production performance compared to undoped TiO_2, as metals provide additional reaction sites and enhance charge separation. The use of bimetallic dopants further optimizes the hydrogen evolution reaction. Additionally, porphyrins, with their strong visible light absorption and efficient electron transfer properties, have demonstrated potential in TiO_2 photocatalysis. Their incorporation expands the photocatalyst's light absorption range into the visible spectrum, enhancing H_2 production efficiency. This review paper explores the principles and advancements in metal- and porphyrin-doped TiO_2 photocatalysts, highlighting their potential for sustainable hydrogen production.

Keywords: hydrogen production; water splitting; photocatalysis; TiO_2; metal doping; porphyrins

check for updates

Academic Editors: Torben R. Jensen, Eleonora Aneggi, Roberto Nisticò and Hicham Idriss

Received: 14 March 2025
Revised: 7 April 2025
Accepted: 7 April 2025
Published: 11 April 2025

Citation: Bitsos, D.R.; Salepis, A.; Orfanos, E.; Coutsolelos, A.G.; Kosheleva, R.I.; Mitropoulos, A.C.; Ladomenou, K. Exploring Metal- and Porphyrin-Modified TiO_2-Based Photocatalysts for Efficient and Sustainable Hydrogen Production. *Inorganics* **2025**, *13*, 121. https://doi.org/10.3390/inorganics13040121

Copyright: © 2025 by the authors. Licensee MDPI, Basel, Switzerland. This article is an open access article distributed under the terms and conditions of the Creative Commons Attribution (CC BY) license (https://creativecommons.org/licenses/by/4.0/).

1. Introduction

Since the beginning of the industrial revolution, there has been a significant challenge in transitioning from coal to liquid fuels [1]. This issue stems from the fact that energy production and consumption do not occur in the same location, leading to geopolitical confrontations and energy losses due to fuel transportation. The first oil crises of the

1970s resulted in high production costs that industrialized countries such as Germany and the United States could not sustain. Consequently, these nations faced embargoes from oil-producing countries due to political and economic disputes. Unlike previous energy crises driven solely by traditional supply and demand forces, the current crisis, which began unofficially in 2020, is unique and complex, influenced by a set of factors specific to our time [2]. One major factor in the recent crisis is the difficult transition to green energy, exacerbated by poorly planned decarbonization efforts. The shift from fossil fuels to renewable energy sources has been hindered by a lack of investment in infrastructure, inadequate statistical forecasting, and inefficient organization of renewable energy resources. As a result, the stable balance between energy production and consumption has been disrupted. Many countries struggle to maintain energy self-sufficiency, while electricity imports contribute to blackouts and rising fossil fuel prices. For instance, the price of natural gas increased by 400% in the first quarter of 2022, and the price of a barrel of oil reached EUR 93—the highest in the past three years [3]. The energy crisis has triggered high inflation, economic slowdowns, and long-term instability, potentially leading to prolonged economic crises and widespread poverty. To address this challenge, energy production technologies must leverage existing distribution systems, be accessible to all countries, and remain environmentally sustainable. One fuel that meets all these criteria is hydrogen [4].

Hydrogen is the lightest and most abundant element in the universe, but it is rarely found on Earth in its pure form. Instead, it is typically found bonded to other elements, such as in water or hydrocarbons. Despite its limited availability in nature, hydrogen is a crucial fuel source with the potential to revolutionize the energy industry. One of hydrogen's key advantages is its clean combustion, producing only water vapor with no greenhouse gas emissions or air pollution. Additionally, hydrogen fuel cells can convert the chemical energy of hydrogen into electricity, with water as the only byproduct [5]. However, hydrogen fuel cells remain relatively expensive, and challenges persist in its production, storage, and transportation [6]. Despite these obstacles, many companies and governments are investing in hydrogen technology as a means to reduce greenhouse gas emissions and transition to cleaner, renewable energy sources [7]. Exploring and developing new hydrogen production methods could pave the way for a cleaner and more sustainable energy future for our planet [8,9].

The advantages of TiO_2, as a photocatalyst, stem from its high chemical stability, abundance, and ability to generate electron–hole pairs under light irradiation. These properties enable TiO_2 to facilitate redox reactions on its surface, making it widely studied for hydrogen production via photocatalysis. However, TiO_2 has a wide bandgap (~3.2 eV for anatase), meaning it primarily absorbs UV light, which accounts for only 5% of the solar spectrum. To improve its efficiency, doping TiO_2 with metals like Pt, Au, Ni, Cu or incorporating metal-based porphyrins, extends its absorption range into the visible spectrum, improves charge separation, and suppresses the recombination of photo-generated electron–hole pairs [10,11]. Porphyrins, organic compounds with a conjugated ring structure, are being explored as potential dopants for TiO_2 due to their ability to absorb light in the visible solar spectrum. Their unique optical and electronic properties, particularly in the Soret and Q bands, make them ideal for enhancing TiO_2's photocatalytic activity beyond the UV range. By transferring energy to TiO_2 semiconductors, porphyrins facilitate efficient solar-driven hydrogen production [12,13]. This review highlights the development of metal- and porphyrin-doped TiO_2 catalysts, which provide additional reaction sites, enhance light absorption and improve charge carrier separation, ultimately boosting photocatalytic hydrogen production.

2. Semiconductor Photocatalysis

Photocatalysis utilizes light energy to accelerate chemical reactions between a catalyst and a substrate. In the context of hydrogen production, a photocatalyst enables the conversion of water into hydrogen and oxygen by generating electron–hole pairs under solar irradiation [14]. The main appeal of this process lies in its potential to produce hydrogen fuel in a clean, sustainable, and cost-effective manner, without releasing harmful emissions [15]. Consequently, the development of efficient and stable photocatalytic materials is a key area of research in renewable energy. Semiconductors play a fundamental role in in this process, acting as the primary photocatalysts. Semiconductors play a pivotal role in this process, acting as the primary photocatalysts. When exposed to light, these materials absorb photon energy, which excites electrons from the valence band to the conduction band, leaving behind positively charged holes in the valence band (Scheme 1).

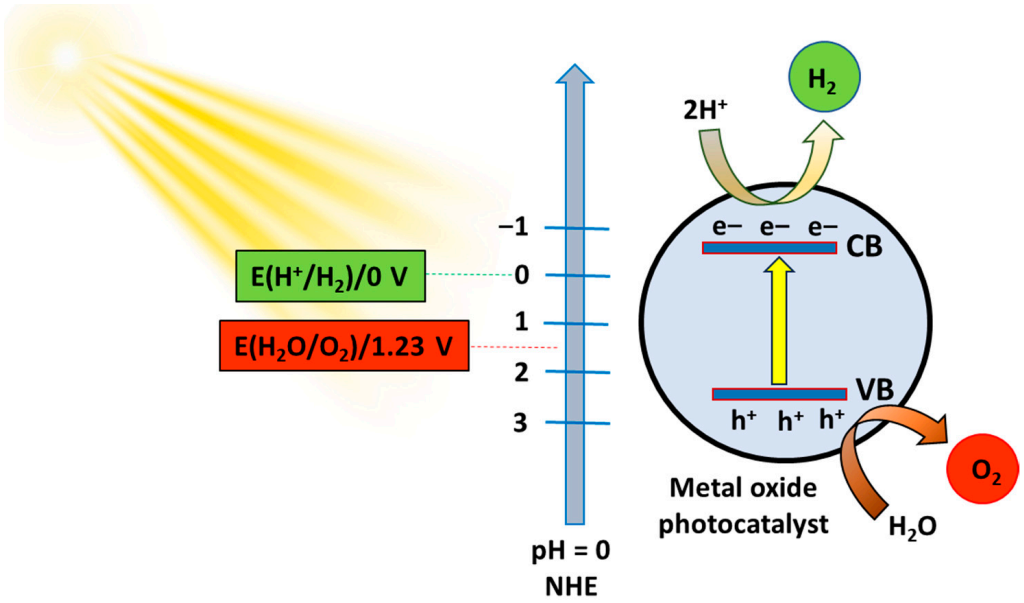

Scheme 1. General scheme of photocatalytic hydrogen production using a metal oxide photocatalyst and a sacrificial electron donor (SED).

The absorption of light is a prerequisite for photocatalytic reactions to proceed [16,17]. For a photon to induce an electronic transition, its energy must match or exceed the energy difference between the ground state and the excited state—a requirement de-fined by the material's bandgap [18]. Upon absorption, an electron is promoted from the ground singlet state (S_0) to an excited singlet state (S_1), where electron spins remain paired. In some cases, intersystem crossing can occur, allowing the molecule to transition into a triplet state (T_1), where the spins are unpaired. Although the triplet state is lower in energy and longer-lived, transitions to it are spin-forbidden and occur less readily. According to selection rules, direct excitation from S_0 to T_1 is not allowed, while excitation from S_0 to S_1 is spin-allowed [19]. The absorption of a photon radiation occurs very quickly. The molecule's energy can be lost by emitting a photon of the same energy (resonance fluorescence) or it can lose its vibrational energy through collisions with neighboring molecules and be degraded to its lowest vibrational level (vibrational relaxation). In semiconductor physics, when a semiconductor is irradiated with photons of equal to or greater than the bandgap energy ($hv \geq EBG$), it is excited, generating an electron–hole pair ($e-/h^+$) [20]. These charge carriers can then migrate to the surface of the semiconductor, where they participate in redox reactions. An internal electric field at the semiconductor–electrolyte interface helps separate the charges, overcoming their mutual Coulombic attraction [21].

Once at the surface, electrons and holes may become trapped near or on the surface of the semiconductor, which can prolong their lifetimes and enhance their reactivity. Once at the surface, electrons and holes may become trapped near or on the surface of the semiconductor, which can prolong their lifetimes and enhance their reactivity [22]. These traps are characterized as follows:

$$e-_{CB} \rightarrow e-_{tr}$$

$$h^{+}{}_{VB} \rightarrow h^{+}{}_{tr}$$

These charge carriers drive the water-splitting reactions, which can occur under both acidic and alkaline conditions. In alkaline media, the reduction half-reaction is as follows:

$$2H_2O + 2e- \rightarrow H_2 + 2OH-$$

In acidic media, often catalyzed by noble metals like platinum, the oxidation half-reaction proceeds as follows:

$$2H_2O \rightarrow O_2 + 4H^{+} + 4e-$$

Together, these reactions facilitate the generation of hydrogen and oxygen gases, providing a pathway to produce hydrogen fuel for energy and industrial uses [12,23,24]. To improve photocatalytic efficiency, semiconductors can be doped with specific elements and engineered to increase their surface area. Such modifications enhance light absorption, charge separation, and surface reactivity. Overall, semiconductors are indispensable in the development of advanced photocatalytic systems for sustainable hydrogen production.

3. Titanium Dioxide as Semiconductor in Photocatalysis

Various semiconductors have been explored for photocatalytic applications. While many demonstrate promising characteristics, their long-term viability is often hindered by high charge recombination rates, poor stability in aqueous environments, or toxicity [25–29]. Among the most studied are n-type semiconductors with wide bandgaps, such as CdS, WO_3, and ZnO (Figure 1) [30,31]. These materials possess favorable conduction and valence band positions for photocatalysis; however, their large energy bandgaps (EBG) necessitate ultraviolet (UV) irradiation for activation. This is a significant limitation, as the majority of solar radiation falls within the visible spectrum (~480 nm), with only a small fraction in the UV range. On the other hand, semiconductors like CdS, CdSe, ZnS, and PbS exhibit narrower bandgaps (~2 eV), enabling excitation by visible light [16,28,32,33]. Despite this advantage, their inherent toxicity and instability in aqueous media severely restrict their practical application in photocatalytic systems.

Titanium dioxide (TiO_2) stands out as one of the most widely utilized photocatalysts due to its non-toxic nature, chemical stability, low cost, and ease of synthesis in various nanostructured forms such as nanoparticles, nanotubes, and nanowires. These morphologies play a significant role in modulating its photocatalytic performance TiO_2 primarily exists in two crystalline phases: anatase and rutile [34,35]. Anatase, with a bandgap of approximately 3.2 eV, features a higher surface area, superior electron mobility, and lower recombination rates, making it more efficient for photocatalysis under UV light. Rutile, although less reactive, exhibits greater thermal stability. Combining anatase and rutile phases, or doping them with metal or non-metal elements, has been shown to enhance charge separation and extend light absorption, thereby improving overall photocatalytic efficiency [36,37]. TiO_2 has been extensively studied for hydrogen generation via water splitting under both UV and visible light conditions [33,38–40]. However, a major limita-

tion is the high recombination rate of photogenerated charge carriers, which reduces the efficiency of the overall process [41,42].

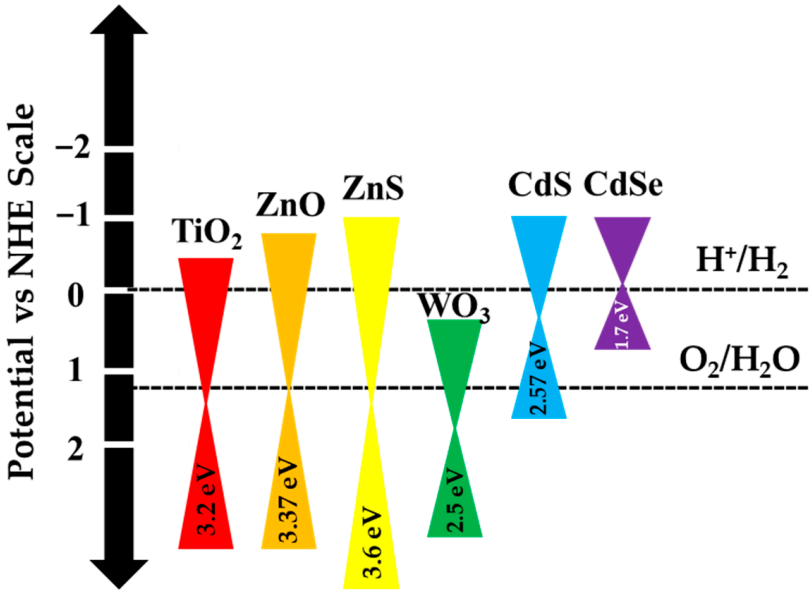

Figure 1. Energy gaps of most well-known semiconductors.

A key mechanism in TiO_2 photocatalysis involves the partial reduction of titanium cations. Under light excitation, Ti^{4+} ions—either on the surface or within the bulk of the material—can trap photogenerated electrons, forming Ti^{3+} species located just below the conduction band [38,40,43]. This process is represented by the following equilibrium:

$$e^{-}_{CB} + Ti^{+4}\,OH \rightleftharpoons Ti^{+3}\,OH$$

This equation describes the trapping of conduction band electrons by surface-bound Ti^{4+} sites, resulting in the formation of Ti^{3+} species slightly below the conduction band edge. These electron traps contribute to extending charge carrier lifetimes, thereby enhancing photocatalytic efficiency, especially when the trapping occurs near the surface, where redox reactions take place.

3.1. The Importance of TiO_2 Modification

TiO_2 possesses several advantageous characteristics as a semiconductor and photocatalyst, making it superior to other available catalysts for photocatalytic reactions [29,39]. However, its relatively large bandgap limits photon absorption efficiency, while the recombination of photo-induced electron–hole pairs further limits its photocatalytic efficiency [10,44,45]. These limitations reduce the overall performance of TiO_2-based systems by contributing to energy losses.

To improve photocatalytic hydrogen production, it is essential to employ strategies that suppress charge carrier recombination and facilitate efficient charge separation and transfer from the catalyst surface to the reactants. Another key aspect is expanding the light absorption range of the material to harness a broader portion of the solar spectrum. For enhanced efficiency and performance, TiO_2-based photocatalysts should have the following abilities:

i. Extend light absorption into the visible region.
ii. Efficiently separate charge carriers and promote their transfer to surface reactants.
iii. Incorporate suitable cocatalysts to boost photocatalytic activity.

Sacrificial agents also play a vital role in photocatalysis by donating electrons to prevent charge carrier recombination, thereby sustaining the photocatalytic process. Organic compounds such as methanol and ethanol are commonly employed as sacrificial agents in hydrogen production. They act as hole scavengers, helping to prolong the active life of the photocatalyst [46]. Moreover, the addition of cocatalysts such as platinum (Pt) or nickel (Ni) on the TiO_2 surface significantly enhances hydrogen evolution. These cocatalysts improve electron transfer, reduce the overpotential required for water splitting, and provide additional active sites for the reaction [47].

3.2. Metal Modification of TiO_2

Transition metals such as Pt, Au, Ag, Ni, and Pd are commonly used in order to modify TiO_2, as their electronic structure allows them to participate in catalytic reactions. These metals have their last electron entering an inner orbital, leaving the outer orbital with two electrons, which enables them to act as additional catalysts for electron trapping [11].

The deposition of metals on TiO_2 is one of the most widely used surface modification techniques to suppress the recombination of photogenerated electron–hole pairs. In practice, metals serve as electron traps, promoting efficient charge separation due to their high work function, which enhances electron acceptance. Metal enrichment can be achieved through various methods without compromising the photocatalyst's performance.

Doping TiO_2 with transition metal nanoparticles has gained significant interest in improving photocatalysis through the surface plasmon resonance (SPR) phenomenon [48,49]. In this process, noble metals such as Au, Pt, and Ag exhibit strong SPR effects in the visible range. At elevated temperatures, the SPR effect is further enhanced, leading to increased photocatalytic activity (Figure 2).

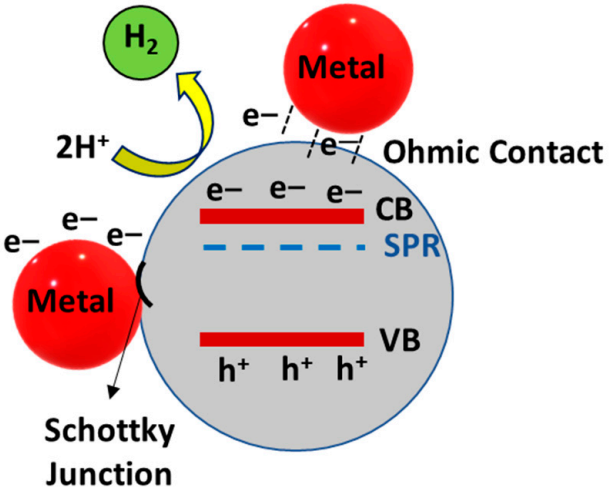

Figure 2. The graph shows the surface plasmon resonance when TiO_2 contacts a metal, forming Schottky junctions and Ohmic contacts (CB: conduction band; VB: valence band; SPR: surface plasmon resonance).

Upon modifying the bandgap of TiO_2 and enhancing its electronic properties, various surface modifications have been implemented, including dye sensitization [50–52], the use of nanocomposites [53–55], and doping with non-metals [56,57] and metals [58]. Among these approaches, metal doping stands out as a superior choice, as it can alter the electronic properties of TiO_2, act as an electron trap, facilitate electron–hole transfer, shift bandgap absorption toward the visible spectrum, and provide additional active sites for photocatalytic hydrogen evolution. Table 1 summarizes the key metal-doped TiO_2 photocatalysts reported in the literature. Composites of noble metals with TiO_2 have been proven to

enhance the photocatalytic activity of titania in H_2 production. In one study, Pt/TiO_2 nanocrystals were synthesized to investigate the impact of Pt loading on photocatalytic performance. The results demonstrated that incorporating Pt significantly improved the hydrogen evolution rate, with 1.0 wt% Pt-loaded Pt/TiO_2 nanocrystals, featuring (001) exposed facets, achieving the highest photocatalytic activity (11.2 mmol $h^{-1}g^{-1}$) (entry 1, Table 1) [59]. Additionally, various platinum composites were deposited on TiO_2 P25 and tested for hydrogen production using methanol as a sacrificial agent.

Table 1. Summary of metal-doped TiO_2 photocatalysts and their hydrogen production efficiencies.

Entry	Photocatalyst	Metal Concentration	Light Source	H_2 Production Efficiency	Reference
1	Pt/TiO_2	1.0 wt% Pt	AM 1.5 G sunlight	11.2 mmol h^{-1} g^{-1}	[59]
2	Pt/TiO_2	5.0 wt% Pt	UV (280–400 nm)	27.6 mmol h^{-1} g^{-1}	[60]
3	Au/TiO_2	2.0 wt% Au	Vis (500 ± 20 nm)	0.05702 mmol h^{-1} g^{-1}	[61]
4	Ag/TiO_2	1.5 wt% Ag	UV (365 nm)	23.5 mmol h^{-1} g^{-1}	[62]
5	Ru/TiO_2	3.0 wt% Ru	UV (280–400 nm)	4.7 mmol h^{-1} g^{-1}	[63]
6	Cu/TiO_2	2.0 wt% Cu	UV (365 nm)	5.0 mmol h^{-1} g^{-1}	[64]
7	Ni/TiO_2	2.0 wt% Ni	UV (365 nm)	2.3 mmol h^{-1} g^{-1}	[64]
8	Ni/TiO_2	5.0 wt% Ni	UV (365 nm)	1.608 mmol $h^{-1}g^{-1}$	[65]
9	Co/TiO_2	2.0 wt% Co	UV (365 nm)	2.25 mmol h^{-1} g^{-1}	[64]
10	Co/TiO_2	1.0 wt% Co	Sunlight	0.22 mmol h^{-1} g^{-1}	[66]
11	Fe/TiO_2	1.1 wt% Fe	UV (250 nm) to visible (750 nm)	0.0155 mmol h^{-1} g^{-1}	[67]
12	$Ni\text{-}Fe/TiO_2$	1 wt% Ni–Fe (1:3)	Sunlight	8.27 mmol h^{-1} g^{-1}	[68]
13	$Ni\text{-}Cu/TiO_2$	1 wt% Ni–Cu (1:1)	UV (365 nm)	186 µL h^{-1} cm^{-2}	[69]
14	$Ag\text{-}Ni/TiO_2$	Ag-Ni (1.5:1.5)	UV (365 nm)	2.9339 mmol h^{-1} g^{-1}	[70]
15	Nb-Ta/TiO_2 (NTTO)	2 wt% Nb and 4 wt% Ta	Simulated solar illumination	1.168 mmol h^{-1} g^{-1}	[71]
16	$Ni\text{-}Pt/TiO_2$	0.01 wt% Ni and 1.0 wt% Pt	15 W black lamp (352 nm)	3.983 mmol g^{-1} h^{-1}	[72]

The structural and electronic properties of the catalysts were analyzed using multiple techniques, revealing that optimizing the platinum–titania interface enhanced photocatalytic performance by approximately 250%, reaching 27.6 mmol $h^{-1}g^{-1}$ (entry 2, Table 1) [60]. The study also identified a synergistic effect between the noble metal and the oxide support at interface sites, which promoted the conversion of carboxylate-type surface species into carbon dioxide and maximized hydrogen production (Figure 3).

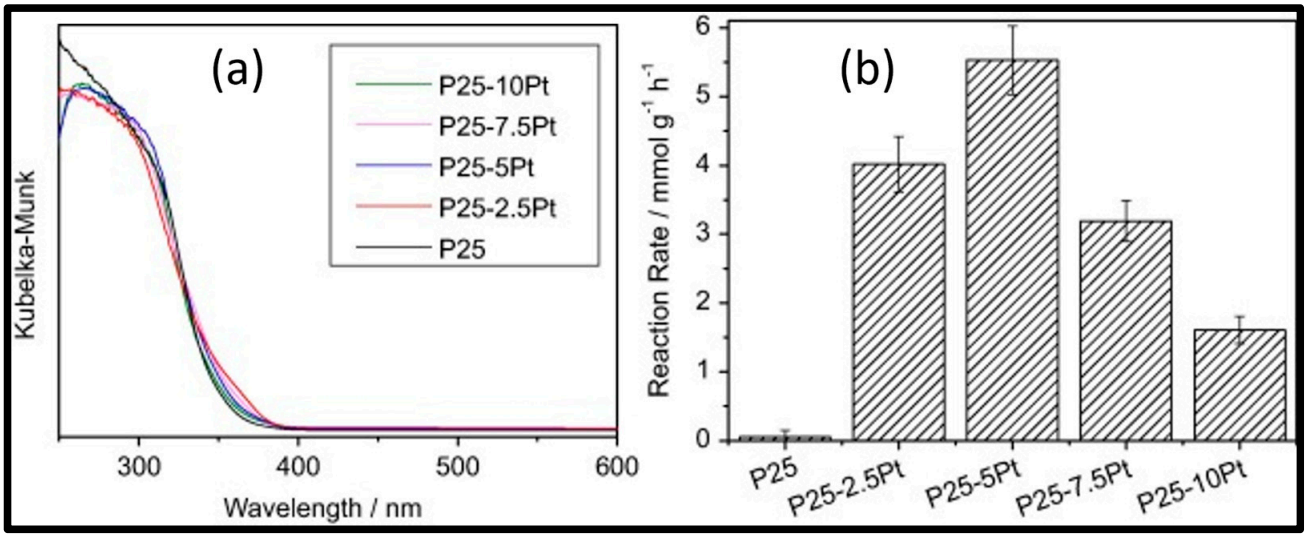

Figure 3. (**a**) UV–visible spectra of Pt and P25 samples (**b**) Hydrogen evolution rate, per gram of catalyst, in the 1:9 CH_3OH: H_2O mixture [60]. Reproduced from ref. [60] with permission from Elsevier, License number 5600041458742.

Gold (Au) has been widely used in photocatalytic hydrogen production due to its plasmonic properties. Au nanoparticles enhance visible light absorption and facilitate electron transfer from the TiO_2 semiconductor to the gold nanoparticles. The charged Au sites provide large surface areas for light stimulation and hydrogen production, significantly improving photocatalytic efficiency when combined with TiO_2 and advancing research toward more efficient photocatalytic systems [73]. A study reported the synthesis of mesoporous plasmonic Au–TiO_2 photocatalysts with varying Au concentrations using a copolymer-assisted sol–gel method [58]. These nanocomposites demonstrated excellent hydrogen production from photocatalytic water reduction under visible light, with 2 wt% Au–TiO_2 exhibiting the highest activity. The proposed mechanism was attributed to three key factors: (i) copolymer-induced defect/impurity states in the TiO_2 matrix, (ii) plasmon excitation of gold nanoparticles, and (iii) plasmon-excited electron transfer from Au nanoparticles to TiO_2, leading to hydrogen generation. The photocatalytic experiments showed hydrogen production rates of 0.05702 mmol $h^{-1}g^{-1}$ under UV-Vis light and 7 µmol $h^{-1}g^{-1}$ under visible light (500 ± 20 nm) (entry 3, Table 1) [61]. Another study explored the development of efficient metal-doped semiconductors for hydrogen production, focusing on Ag-doped TiO_2 photocatalysts synthesized through a cost-effective chemical reduction method. These catalysts exhibited a high hydrogen production rate of 23.5 mmol g^{-1} h^{-1} (entry 4, Table 1) with a quantum yield of 19%, attributed to the presence of oxygen vacancies and the Ti-Ag-O phase. The study also investigated the effects of reaction time, photocatalyst dosage, and sacrificial agents on the water-splitting process, providing valuable insights into the strategic design of metal–support hybrid configurations for photocatalytic hydrogen production [62]. The role of ruthenium (Ru) in TiO_2-based photocatalysts was also examined for hydrogen evolution. A series of Ru/TiO_2 catalysts were tested under UV and visible light irradiation in methanol–water mixtures (entry 5, Table 1) [63]. To further enhance TiO_2's photocatalytic performance for hydrogen production, researchers developed low-cost M/TiO_2 semiconductor catalysts using the impregnation method (Figure 4c). This involved depositing five different first-row transition metals (Fe, Co, Ni, Cu, or Zn) onto a commercially available TiO_2 support. The photocatalytic activity of these M/TiO_2 catalysts was investigated under UV (Figure 4b) and visible light irradiation (Figure 4a), with a metal loading of 2 wt%. Among them, Cu/TiO_2 (Figure 4d) demonstrated the highest hydrogen production efficiency, with rates of approximately 5.0 mmol $h^{-1}g^{-1}$ under UV irradiation and 0.22 mmol $h^{-1}g^{-1}$ under visible light irradiation (entry 6, Table 1) [64]. These values were significantly higher than those obtained with undoped TiO_2 (Figure 4d), by factors of 16 and 3 for UV and visible light, respectively. Copper-doped TiO_2 (Cu-TiO_2) is commonly used for photocatalytic hydrogen production due to the following: (i) increased electron–hole separation: Copper doping enhances charge separation, reducing recombination and leading to more efficient hydrogen production [64]; (ii) enhanced light absorption: Cu doping extends TiO_2's light absorption into the visible region, improving its ability to utilize sunlight for photocatalysis; iii) stability: Cu-TiO_2 has been found to be stable under photocatalytic conditions, making it a viable material for long-term hydrogen production [64].

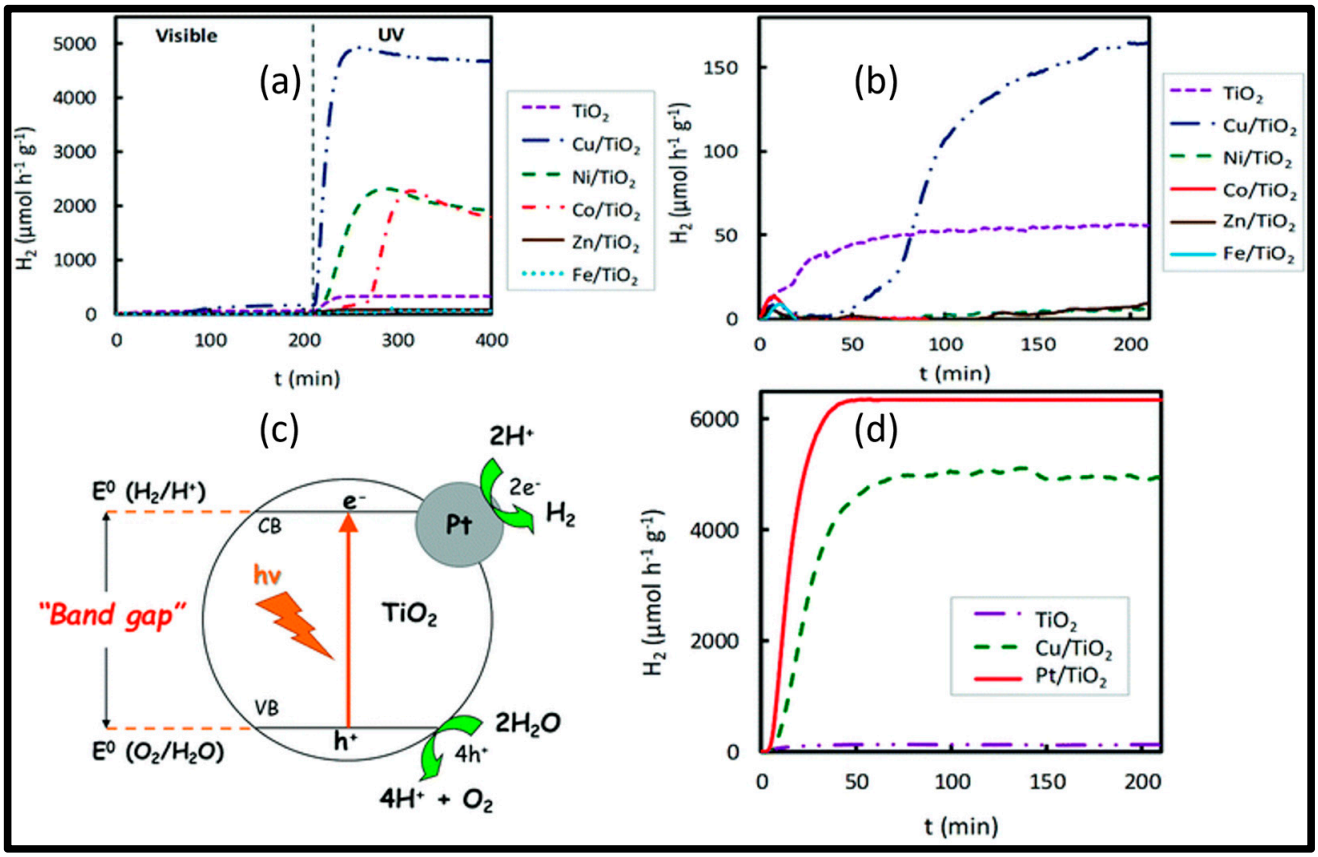

Figure 4. Hydrogen production for impregnated M/TiO_2 photocatalysts (M = Fe, Co, Ni, Cu, Zn), 2 wt% M; (**a**) under both visible and UV light irradiation, (**b**) under visible lamp irradiation, (**c**) schematic diagram of the water-splitting reaction on Pt/TiO_2 and (**d**) comparison of the catalytic activity of bare commercial TiO_2, 2 wt% Cu/TiO_2 and 2 wt% Pt/TiO_2 in the hydrogen photoproduction under UV irradiation. Reproduced from ref. [64] with permission from the Royal Society of Chemistry.

In addition, Ni/TiO_2 and Co/TiO_2 photocatalysts demonstrated high rates of H_2 production under UV light, with values of 2.3 mmol h^{-1} g^{-1} (entry 7, Table 1) and 2.25 mmol h^{-1} g^{-1}, (entry 9, Table 1), respectively (Figure 4a) [64]. Compared to other noble metal-based photocatalysts, such as Pt or Au, Ni is a more cost-effective material, making Ni-TiO_2 an attractive option for large-scale hydrogen production. A study investigated the use of titania nanotubes (NTs) prepared by rapid breakdown anodization for hydrogen generation via water splitting. The NTs were sensitized with platinum (Pt), palladium (Pd), and nickel (Ni) nanoparticles (NPs) to assess their efficiency for water splitting. The metal NPs were deposited on the TiO_2 NTs via chemical reduction. The TiO_2 NTs had a bundled morphology, while the metal NPs appeared as spherical deposits. The addition of metal NPs increased H_2 generation, with lower NP deposits producing better results. Ni NPs had the highest H_2 generation rate among the tested metals. The 5% Ni/TiO_2 NTs had a H_2 value rate of 1.608 mmol h^{-1} g^{-1} under 365 nm UV light (entry 8, Table 1) [65]. In another report, cobalt-doped TiO_2 photocatalysts were synthesized and studied towards hydrogen production. The cobalt-doped TiO_2 showed a maximum hydrogen evolution of 0.22 mmol h^{-1} g^{-1} (entry 10, Table 1) in pure water under solar irradiation. The study systematically investigated various reaction parameters such as the amount of cobalt on TiO_2, glycerol concentration, substrate effect (alcohols), and pH of the solution. Under UV irradiation, a 3- to 4-fold increase in activity was observed initially, but the activity diminished over time due to the loss of cobalt ions. However,

under solar irradiation, the cobalt-doped TiO_2 photocatalysts showed stable and continuous activity [66]. In a following report Fe-ion-doped TiO_2 thin films were studied towards photocatalytic water-splitting under visible light irradiation. The study showed that low concentration metal ion doping near the conducting indium tin oxide (ITO)–TiO_2 interface was important to avoid the formation of recombination centers. The H_2 production rate was higher for Fe-doped TiO_2 compared to undoped TiO_2 due to the ability of Fe ions to trap both electrons and holes [67]. The study also found that TiO_2 films produced a constant H_2 generation rate 0.0155 mmol h^{-1} g^{-1} (entry 11, Table 1) for long periods of time, eliminating the back-reaction effect [67]. Even though there are some earth abundant metals doped on TiO_2 that achieve great H_2 evolution, on average the performances of the noble metals are higher. In order to improve the catalytic performance of non-noble metals, bimetallic systems such as Ni-Fe [68] (entry 12, Table 1) and Ni-Cu [69] were prepared and studied as photocatalysts. The TiO_2 doped with bimetallic catalysts showed enhanced photocatalytic activity compared to the single cocatalysts. For example, the TiO_2 nanotubes coated with Ni-Cu (1:1 atomic ratio) reached 186 μL h^{-1} g^{-1} (entry 13, Table 1) hydrogen evolution rate, which was 4.6 and 3 times higher compared to Ni/TiO_2 and Cu/TiO_2, respectively. Therefore, the bimetallic layers are able to provide synergistic effect and enhance H_2 evolution compared to monometallic-doped TiO_2. In a following example, Ni is deposited on Ag surface to form a core–shell Ag-Ni nanostructure which was used to synthesize Ag-Ni/TiO_2 photocatalyst via one-step photo-induced deposition method [70]. The Ag-Ni/TiO_2 (1.5:1.5) photocatalyst displayed a photocatalytic activity of 2.9339 mmol $h^{-1}g^{-1}$, about 79 times more than TiO_2 (entry 14, Table 1). Continuing with bimetallic catalysts, Nb-Ta co-doped TiO_2 (NTTO) (entry 15, Table 1) nanoparticles achieved a hydrogen evolution rate of 1.168 mmol h^{-1} g^{-1} under simulated solar illumination. This performance, while lower than noble metal-doped systems (e.g., Pt/TiO_2 at 27.6 mmol h^{-1} g^{-1} in entry 2, Table 1), surpasses several non-noble metal-doped catalysts (e.g., Fe/TiO_2 at 0.0155 mmol h^{-1} g^{-1} in entry 11, Table 1). The NTTO nanoparticles leverage dual doping with Nb and Ta to reduce the bandgap (2.90 eV vs. 3.27 eV for undoped TiO_2) and suppress electron–hole recombination by 30%, as demonstrated by photoluminescence studies. This bandgap engineering enhances visible light absorption and charge carrier separation, though the absence of a noble metal cocatalyst limits its efficiency compared to Pt- or Au-based systems. Nevertheless, NTTO's stability and scalable synthesis under mild conditions highlight its potential for sustainable applications. The Nb-Ta/TiO_2 system, while innovative in bandgap tuning, highlights the trade-off between noble metal free design and catalytic efficacy, emphasizing that dual-metal strategies involving noble metals remain pivotal for maximizing H_2 evolution rates [71]. In contrast, Ni-Pt/TiO_2 (entry 16, Table 1) achieves a significantly higher hydrogen evolution rate of 3.983 mmol h^{-1} g^{-1} under UV light (352 nm), outperforming most non-noble metal-doped catalysts (e.g., Cu/TiO_2 at 5.0 mmol h^{-1} g^{-1} in entry 6, Table 1) and even some noble metal systems (e.g., Ru/TiO_2 at 4.7 mmol h^{-1} g^{-1} in entry 5, Table 1). The study investigated various metals (Ag, Cu, Pd) co-deposited with Pt on TiO_2 for photocatalytic hydrogen production. **Ag/Pt** underperformed due to Ag's low work function (4.26 eV), which caused electron backflow from TiO_2 to Ag, reducing charge separation efficiency. Higher Ag loading further hindered performance by blocking light and active sites. **Cu/Pt** showed moderate improvement (1.25× higher H_2 than Pt/TiO_2) at 0.01 wt% Cu, as Cu's work function (4.65 eV) aligned with TiO_2, enabling a weak Schottky junction. However, excess Cu obscured active sites and filtered light. **Pd/Pt** had a high work function (5.12 eV) but lower H_2 yield than Ni/Pt, likely due to less effective synergy in charge transfer or unfavorable hydrogen evolution potential. **Ni/Pt** outperformed others due to Ni's high work function (5.25 eV) and redox synergy with Pt. Pt deposits first (higher redox potential: 1.44 V vs. Ni's −0.257 V), forming

a Schottky junction that traps electrons, while Ni prolongs charge carrier lifetime. Optimal Ni loading (0.01 wt%) avoided site blockage and light obstruction, achieving 341× higher H_2 than pure TiO_2. The Ni-Pt interface facilitated efficient electron transfer and suppressed recombination, surpassing the limitations of Ag, Cu, and Pd in balancing Schottky effects, redox dynamics, and catalyst dispersion. The superior performance of Ni-Pt/TiO_2 arises from the synergistic interplay between Ni and Pt. Platinum, with its high work function (5.65 eV), forms a Schottky junction with TiO_2 (4.2–4.5 eV), effectively trapping photogenerated electrons and reducing recombination. Simultaneously, Ni enhances electron migration from Pt to Ni, prolonging charge carrier lifetimes and providing additional active sites. The optimal loading (0.01 wt% Ni and 1.0 wt% Pt) balances light absorption and catalytic site availability while preventing $Ni(OH)_2$ formation—a common issue in Ni-doped systems. The dominance of Ni-Pt/TiO_2 over other bimetallic systems (e.g., Ni-Cu/TiO_2 at 186 μL h^{-1} cm^{-2} in entry 13 or Ag-Ni/TiO_2 at 2.9339 mmol h^{-1} g^{-1} in entry 14, Table 1) underscores the critical role of Pt's low overpotential for H^+ reduction and its ability to stabilize Ni in metallic form. While non-noble metals like Cu or Ni improve cost-effectiveness, their lower work functions and higher recombination rates limit efficiency. Noble metals like Au (entry 3, Table 1: 0.057 mmol h^{-1} g^{-1}) or Ag (entry 4, Table 1: 23.5 mmol h^{-1} g^{-1}) exhibit strong plasmonic effects but face scalability challenges. Ni-Pt/TiO_2 strikes a balance by combining Pt's electron-trapping efficiency with Ni's affordability and structural benefits, making it a superior choice for high-performance, scalable photocatalytic hydrogen generation [72].

4. Porphyrin-Doped TiO_2 for Photocatalytic Hydrogen Production

Porphyrin-doped TiO_2 has emerged as a promising material for photocatalytic hydrogen production due to its ability to enhance light absorption and charge separation. Porphyrins, with their strong absorption in the visible spectrum, extend TiO_2's photocatalytic activity beyond the UV range, making better use of solar energy. Their interaction with TiO_2 facilitates efficient charge transfer, reducing recombination losses and improving hydrogen generation efficiency [74]. This modification offers a sustainable approach to solar-driven water splitting, advancing the development of clean energy technologies.

Porphyrins are organic molecules consisting of four pyrrole rings interconnected by methine bridges (-CH=), forming a highly conjugated system with 22 π-electrons, 18 of which contribute to its aromatic stability and planar geometry through sp^2 hybridization. This extensive conjugation allows porphyrins to strongly absorb visible light, making them highly effective photosensitizers. Their absorption spectrum includes the Soret band (400–450 nm) and Q bands (500–700 nm), which enhance visible light capture. Additionally, porphyrins can be functionalized with various substituents, allowing the fine-tuning of their electronic and optical properties. When incorporated into a TiO_2 photocatalytic system, porphyrins improve spectral response, enhance electron transfer efficiency, and provide stability under reaction conditions [75–79]

The Soret and Q bands are key features of porphyrins' electronic spectra, making them highly effective as photosensitizers in photocatalytic applications [80,81]. The Soret band, also known as the B band, appears in the 400–450 nm range, typically in the blue region of the visible spectrum. This strong absorption results from an electronic transition in the porphyrin molecule, often from the ground state to an excited singlet state, and is attributed to the $\pi \rightarrow \pi^*$ transition within the highly conjugated porphyrin ring. This enables porphyrins to capture high-energy visible light photons, which are then transferred to TiO_2, enhancing photocatalytic activity.

The Q bands, occurring in the 500–700 nm range (red region of the visible spectrum), are weaker than the Soret band and result from lower-energy $\pi \rightarrow \pi^*$ transitions. These bands are split into multiple peaks due to asymmetry in electron distribution, particularly in

metal-free porphyrins. Despite their lower intensity, the Q bands significantly contribute to visible light absorption, extending TiO_2's light capture into the red region of the spectrum. Together, these absorption bands enable porphyrins to harness a broad range of solar energy, facilitating efficient charge transfer and enhancing hydrogen production [13,82,83].

4.1. Mechanism of Hydrogen Production in Porphyrin-Doped TiO_2 Systems

In porphyrin-doped TiO_2 systems, photocatalytic hydrogen production relies on the efficient separation of charge carriers (electrons and holes) generated under visible light. The mechanism typically involves three main steps: light absorption, electron transfer and hole scavenging and redox reactions. Porphyrins, with their extensive π-conjugated systems, strongly absorb visible light (400–700 nm). The excited electron is transferred to the conduction band of TiO_2 (Scheme 2), enabling TiO_2 to utilize visible light, which it normally cannot absorb. These conduction band electrons participate in water reduction to generate hydrogen (H_2), while the holes remain in the porphyrin molecule. To prevent electron–hole recombination, a sacrificial agent—typically an electron donor such as methanol or ethanol—quenches the hole in the porphyrin (Scheme 2). This maintains charge separation, ensuring continuous hydrogen production. Additionally, cocatalysts like platinum (Pt) can enhance electron transfer and improve hydrogen evolution efficiency. Porphyrins play a crucial role in extending TiO_2's light absorption into the visible spectrum, which accounts for approximately 43% of solar radiation. This significantly enhances the photocatalytic efficiency of hydrogen production [14,77–79,81].

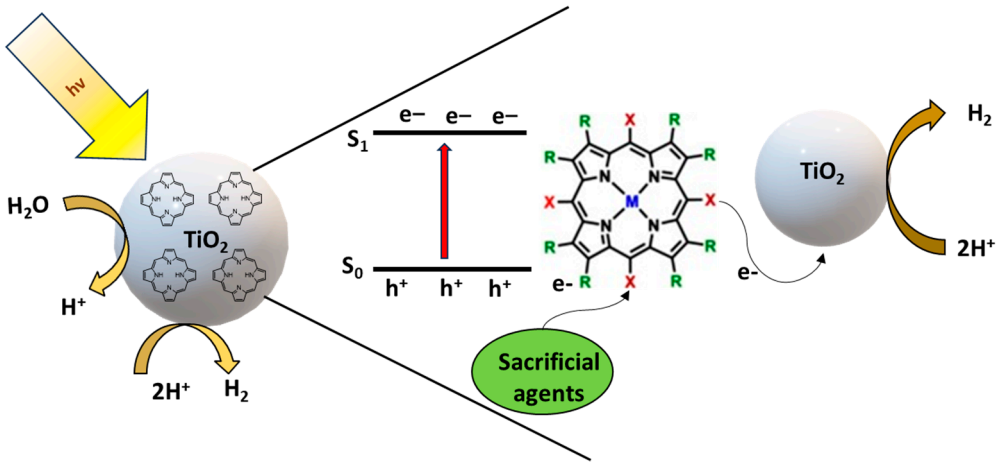

Scheme 2. Photocatalytic hydrogen production and water splitting capabilities of a porphyrin-doped TiO_2 photocatalyst using a sacrificial agent.

4.2. Types of Porphyrins and Their Suitability

Porphyrin-based systems offer extensive tunability through structural modifications. By incorporating different transition metal centers (e.g., Zn, Cu, Co) or functional groups (e.g., carboxylate, phosphonate), their photophysical properties can be tailored for specific applications. Free-base porphyrins, such as tetraphenylporphyrin (H_2TPP), are widely used due to their simple synthesis and tunability; however, they typically exhibit lower stability and electron transfer efficiency compared to metal porphyrins. Among metal porphyrins, zinc porphyrins (ZnTPP) are among the most studied for TiO_2 doping, as they offer strong visible light absorption and efficient electron transfer, making them highly effective for hydrogen production. Copper and cobalt porphyrins have also been explored for their redox properties, providing a balance between cost and performance [84]. Functionalized porphyrins, which incorporate groups such as carboxyl or phosphonic acids, exhibit enhanced binding affinity to the TiO_2 surface. These functional groups facilitate

strong anchoring, ensuring efficient charge transfer between the photosensitizer and the semiconductor while preventing porphyrin aggregation, thereby preserving their optical and electronic properties [80,81]. Furthermore, porphyrins can act synergistically with metallic cocatalysts such as platinum, enhancing hydrogen evolution by improving electron transfer kinetics at the TiO_2 interface. These advantages establish porphyrin-doped TiO_2 as a promising material for sustainable solar-to-hydrogen conversion, positioning it as an efficient and versatile candidate for future energy applications [12,51,54].

4.3. Recent Examples of Porphyrin-Doped TiO_2 Systems for Hydrogen Production

Zinc and platinum porphyrins are among the most studied due to their strong visible light absorption and efficient electron transfer capabilities [52,78,79,82,85]. Functionalized porphyrins, particularly those with carboxyl groups, exhibit enhanced stability and binding efficiency, leading to higher hydrogen production rates [78]. Additionally, high-intensity light sources (e.g., 300 W and 450 W Xenon lamps) significantly increase hydrogen yields, emphasizing the importance of photon energy in photocatalysis [77–79,85,86]. Table 2 presents studies on porphyrin-doped TiO_2 photocatalysts for H_2 production.

Table 2. Summary of porphyrin-Doped TiO_2 photocatalysts and their hydrogen production efficiencies.

Entry	Photocatalyst	Porphyrin	Light Source	H_2 Production Efficiency	Reference
1	Pt/TiO_2-Pt-Tc3CP	Pt-Tc3CP	40 W white LED	707 mmol g^{-1} h^{-1}	[82]
2	Pt-TiO_2 NPs-Zn-TM(pCOOH)P	ZnTM(pCOOH)P	40 W white LED	1959 mmol g^{-1} h^{-1}	[83]
3	PdTCP and PtTCP-TiO_2	PdTCP and PtTCP	visible light irradiation ($\lambda > 420$ nm)	30,200 µmol g^{-1}	[52]
4	Pt/TiO_2-THPP-Pd	THPP-Pd	visible light irradiation ($\lambda > 420$ nm)	2025.4 µmol g^{-1} h^{-1}	[13]
5	TiO_2 MS-Cu-TCPP	TCPP-Cu	300 W Xenon	1.3 mmol g^{-1} h^{-1}	[77]
6	Pt/TiO_2-(LG-5)	Zinc–porphyrin dye (LG-5)	450 W Xenon	4196 mmol g^{-1} h^{-1}	[78]
7	Pt–TiO_2-PCT-LG-23	Zinc-PCT-LG-23	300 W Xenon	9793.5 µmol g^{-1} h^{-1}	[79]
8	TiO_2/ZnTmMpHPP + 0.5%Pt	ZnTmMpHPP	300 W Xenon	326.3 µmol h^{-1}	[85]
9	THPP-TiO_2-H NPs	THPP	UV cutoff filter > 400 nm	4.80 mmol g^{-1}	[87]
10	TiO2/Co/PA	TCPP	300 W xenon lamp	4318.4 µmol g^{-1} h^{-1}	[86]

Firstly, the Pt/TiO_2 with Pt-Tc3CP (entry 1, Table 2) system, using platinum tetraphenylporphyrin (Pt-Tc3CP) as a photosensitizer paired with TiO_2, achieved a hydrogen production rate of 707 mmol g^{-1} h^{-1} under a 40 W white LED. This high yield demonstrates the effectiveness of platinum porphyrins in extending TiO_2's light absorption into the visible spectrum. Platinum cocatalysts stabilize photogenerated electrons, enhancing charge separation and reducing recombination losses. This synergy between porphyrin sensitization and platinum's catalytic activity underpins the system's impressive performance [82]. Zn-TM(pCOOH)P on Pt-TiO_2 (entry 2, Table 2) achieves a hydrogen evolution rate of 1959 mmol g^{-1} h^{-1}, highlighting the effectiveness of zinc porphyrins functionalized with carboxyl groups. These groups enhance binding to TiO_2 surfaces, improving light harvesting and charge transfer. The interaction between zinc porphyrins and TiO_2 minimizes energy loss during electron transfer, optimizing performance [83]. The PdTCP and PtTCP-TiO_2 (entry 3, Table 2) configuration delivers an exceptional 30,200 µmol g^{-1} of hydrogen under visible light ($\lambda > 420$ nm). The combined use of palladium (Pd) and platinum (Pt) tetraphenylporphyrins maximizes photocatalytic activity by leveraging Pd and Pt's unique electron affinities, facilitating rapid charge separation. The tetraphenylporphyrin structure aids light absorption and stabilizes photogenerated carriers, posi-

tioning this system as one of the most effective in the table [52]. Palladium-substituted tetraphenylporphyrin (THPP-Pd), when combined with Pt/TiO_2 (entry 4, Table 2), achieves a hydrogen evolution rate of 2025.4 μmol g^{-1} h^{-1} under visible light. This setup highlights the importance of palladium's catalytic properties in reducing overpotentials for hydrogen generation while enabling better charge mobility. The palladium component works synergistically with the porphyrin sensitizer and TiO_2 to deliver reliable photocatalytic performance [13]. Copper–tetraphenylporphyrin (TCPP), integrated into TiO_2 modified structures (MS-TiO_2) (entry 5, Table 2), achieves a modest hydrogen production rate of 1.3 mmol g^{-1} h^{-1} under 300 W xenon light. Copper functions as an efficient redox catalyst, aiding electron mobility and improving water-splitting reactions. However, its lower performance compared to Pt and Pd systems indicates the need for optimization in porphyrin–TiO_2 interactions [77]. The zinc–porphyrin dye (LG-5) system (entry 6, Table 2), which achieves 4196 mmol g^{-1} h^{-1} under a 450 W xenon lamp, demonstrates remarkable photocatalytic activity. The strong absorption of visible light by the zinc dye and efficient energy transfer to TiO_2 contribute to the high hydrogen evolution rate, showcasing the potential of zinc porphyrins in high-intensity light applications [78]. Zn-PCT-LG-23 on TiO_2 (entry 7, Table 2) produced 9793.5 μmol g^{-1} h^{-1}, highlighting the impact of advanced porphyrin structural modifications on hydrogen production. These modifications enhance light absorption and charge transfer efficiency, enabling higher performance under 300 W xenon light. The system's success emphasizes the importance of fine-tuning porphyrin structures for optimized photocatalytic activity [79].The ZnTmMpHPP on TiO_2 with 0.5% Pt (entry 8, Table 2) system achieves a moderate hydrogen production rate of 326.3 μmol h^{-1} under xenon light. Although the zinc porphyrin (ZnTmMpHPP) sensitizer contributes to visible light absorption, the efficiency is limited compared to other systems due to weaker porphyrin–TiO_2 interactions and possible electron–hole recombination. The addition of platinum as a cocatalyst stabilizes photogenerated electrons, but further optimization is needed to enhance hydrogen evolution [85].The incorporation of two novel porphyrin-doped TiO_2 systems, THPP-TiO_2-H NPs (entry 9, Table 2) [87] and TiO_2/Co/PA (entry 10, Table 2) [86], underscores significant advancements in addressing TiO_2's limitations for photocatalytic hydrogen production. The THPP-TiO_2-H NPs system (entry 9, Table 2) leverages a hybrid microstructure combining meso-tetra(4-hydroxyphenyl) porphyrin (THPP) with anatase-phase TiO_2, achieving a hydrogen evolution rate of 4.80 mmol g^{-1} h^{-1} under visible light ($\lambda > 400$ nm). This performance arises from the intimate interfacial contact between THPP and TiO_2, which enhances charge transfer efficiency, while the hydrothermal treatment ensures high crystallinity of TiO_2, reducing electron–hole recombination. The system's scalability (up to 500 mL synthesis) further highlights its practical potential. However, its moderate efficiency compared to noble metal-coordinated systems like Zn-TM(pCOOH)P/TiO_2 (entry 2, Table 2: 1959 mmol g^{-1} h^{-1}) or PdTCP/TiO_2 (entry 3, Table 2: 30,200 μmol g^{-1}) suggests limitations in the absence of Pt/Pd co-catalysts, which are critical for stabilizing photogenerated electrons and optimizing light utilization [87]. In contrast, the TiO_2/Co/PA nano–micro hybrid PA (entry 10, Table 2) introduces cobalt ions as interfacial anchors to immobilize J-type porphyrin assembly (PA) derived from CuTCPP, achieving 4318.4 μmol g^{-1} h^{-1} under a 300 W xenon lamp. The cobalt-mediated anchoring minimizes the H-aggregation of PA, ensuring uniform distribution and enhanced electron transfer, while the hybrid's dual functionality—efficient methylene blue degradation alongside H_2 production—demonstrates its versatility. Notably, the system's stability in mixed sacrificial agents (methanol/TEOA) addresses a common challenge in porphyrin-based photocatalysts. Despite these strengths, its performance remains lower than Pt- or Pd-doped systems (e.g., entry 3, Table 2), likely due to the reliance on cobalt rather than noble metals and the use of a xenon lamp rather than optimized visible light sources [86].

Both systems exemplify the critical role of structural engineering (hybrid/nano–micro architectures) and co-catalyst integration (Co^{2+}) in improving charge separation and light absorption. However, they also highlight the persistent efficiency gap between noble metal-free systems and their noble metal-doped counterparts. These findings reinforce the need for future research to optimize porphyrin–metal interactions, explore low-cost co-catalysts (e.g., Ni, Cu), and scale visible light-driven designs to achieve competitive efficiencies while maintaining sustainability. Collectively, these entries advance the field by demonstrating how material innovation and strategic co-catalyst use can balance performance, stability, and practicality in photocatalytic hydrogen production. The versatility of porphyrins in adapting to diverse architectures—from hybrid nanocomposites to hierarchical nano–micro structures—is a key strength highlighted in these systems. For instance, the THPP-TiO_2-H NPs exemplify how porphyrins can be tailored for self-assembly into TiO_2 matrices [87], while the TiO_2/Co/PA showcases their integration into complex heterostructures via metal coordination [86]. This adaptability extends beyond TiO_2-based systems; porphyrins are widely incorporated into metal–organic frameworks (MOFs) [88], nanoparticles (NPs) [89], and core–shell designs, where their tunable electronic properties and strong visible light absorption enhance photocatalytic performance. In MOFs, porphyrins act as light-harvesting nodes [90], while in NPs [91], their conjugation with semiconductors improves charge separation. The reviewed systems align with this broader trend, demonstrating how strategic porphyrin functionalization (e.g., carboxyl or hydroxyl groups) enables robust anchoring and interfacial electron transfer across varied platforms. Reported hydrogen production rates vary widely, from 326.3 μmol h^{-1} to 30,200 μmol g^{-1}, depending on the porphyrin structure, light source, and cocatalysts [52,85]. The differences in photocatalytic performance highlight the need for optimized porphyrin design and integration with TiO_2 to maximize light absorption and minimize recombination losses. High-performing systems, such as PdTCP (entry 3, Table 2) and Zn-TM (pCOOH)P (entry 2, Table 2), are excellent examples due to optimized structural features, effective cocatalysts, and strong porphyrin–TiO_2 interactions [52,83]. In contrast, lower-performing systems suffer from weaker [52,85] binding, suboptimal light absorption, and less efficient cocatalysts. Several key factors influence the efficiency of porphyrin-doped TiO_2 photocatalysts. The molecular structure of the porphyrin (Figure 5) and the presence of functional groups, such as carboxyl, determine binding strength with TiO_2. Cocatalysts, particularly noble metals like Pt and Pd, enhance catalytic activity by stabilizing photogenerated electrons and lowering the energy required for hydrogen evolution. Less effective cocatalysts, such as copper, generally result in reduced performance [77]. Additionally, porphyrins optimized for broad-spectrum light absorption—especially under high-intensity light—demonstrate superior photocatalytic activity. The strength of porphyrin–TiO_2 interactions, often influenced by functionalization, plays a crucial role in ensuring efficient electron transfer and reducing recombination losses. Systems with weak porphyrin–TiO_2 interactions tend to exhibit lower hydrogen production rates. Ultimately, achieving high photocatalytic efficiency requires a balance between effective charge carrier utilization and minimized recombination. Systems that integrate strong porphyrin sensitization, efficient cocatalysts, and structural modifications demonstrate superior performance, underscoring the importance of optimizing both structural (Figure 5) and operational parameters [79,83]. These findings underscore the importance of structural and operational factors in determining the performance of porphyrin-doped TiO_2 photocatalysts.

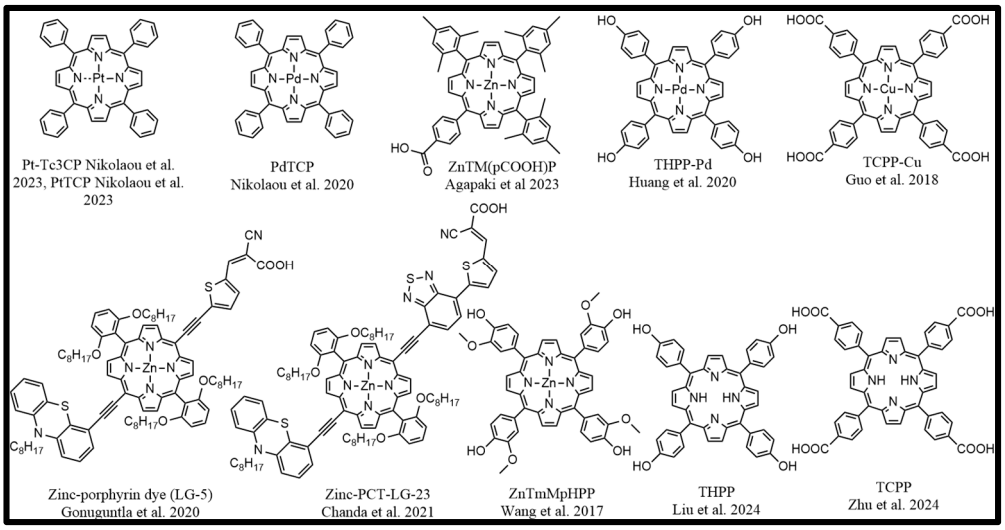

Figure 5. Molecular structure of the porphyrins [13,52,77–79,83,85–87].

4.4. Drawbacks and Challenges of Porphyrin-Doped TiO_2 Systems for Hydrogen Production

Despite the promising benefits, several challenges hinder the maximization of efficiency and scalability in porphyrin-doped TiO_2 systems for hydrogen production. A primary concern is the photostability of porphyrins, which are susceptible to photodegradation (or photobleaching) under extended light exposure. This degradation leads to a decrease in photocatalytic activity over time, limiting the feasibility of these systems for continuous hydrogen production. Strategies for stabilization, such as using metal-centered porphyrins or functionalized porphyrin derivatives, are being explored to improve durability in photocatalytic applications. Another key issue is electron–hole recombination. While porphyrins enhance TiO_2's light absorption, recombination of photogenerated charge carriers remains a challenge. To address this, sacrificial agents or additional cocatalysts are often required, adding complexity and cost to the system. Furthermore, porphyrin molecules tend to aggregate on the TiO_2 surface, potentially reducing light absorption and charge transfer efficiency. Managing porphyrin loading and dispersion on TiO_2 is critical to maintaining optimal performance. Finally, the cost of metal porphyrins, particularly those containing platinum or other noble metals, poses an economic challenge for large-scale applications. Alternatives such as copper or zinc porphyrins are being investigated to reduce costs, although their performance and stability still require further evaluation [77–79,83,85].

5. Conclusions

In this review, we have highlighted recent advances in the use of metal-doped and porphyrin-doped TiO_2 for photocatalytic hydrogen production. Our focus has been on the impact of both monometallic dopants (e.g., Pt, Au, Cu, Ni, Co, Ru, Fe, and Ag) and bimetallic dopants (e.g., Ni-Fe, Ni-C, Nb-Ta, and Ni-Pt). Metal doping has emerged as a promising strategy for enhancing charge carrier separation on the TiO_2 surface and shifting light absorption from the UV to the visible spectrum, thus improving overall photocatalytic efficiency under sunlight. However, a significant challenge remains in the development of low-cost, readily available dopants. While metals like Pt and Au are among the most effective, their high-cost limits scalability. The integration of porphyrins as sensitizers or dopants onto TiO_2 has also shown considerable potential for visible light-driven hydrogen production. Porphyrins' strong visible light absorption and electron transfer capabilities enable TiO_2 to efficiently harvest solar energy and produce hydrogen. Despite this potential, challenges such as porphyrin stability under extended illumination and the need to control molecular aggregation remain. Continued research on functionalized

porphyrins and optimized anchoring methods could further enhance the effectiveness and stability of these systems.

6. Future Perspectives and Environmental Considerations

Looking ahead, challenges for metal-doped TiO_2 include economic viability and environmental sustainability. While noble metals like Pt and Au provide superior performance, their high-cost limits scalability. Future research should focus on cost-effective, earth-abundant metals (e.g., Fe, Ni, Cu) and safer, non-toxic alternatives to prevent environmental contamination. Additionally, attention should be given to reducing the environmental impact of metal leaching during photocatalysis, ensuring that these materials are both efficient and sustainable. Developing stable photocatalysts that balance efficiency, cost, and environmental safety will be key for advancing sustainable hydrogen production. To fully realize the potential of TiO_2-based photocatalysts, future studies should focus on creating stable materials with improved surface areas and reduced charge recombination sites. Moreover, optimizing metal and porphyrin deposition methods will be critical for enhancing hydrogen production efficiency and selectivity. Future studies should also prioritize sustainable synthesis methods for porphyrins, ensuring that the materials used are not only effective but also eco-friendly. Expanding the use of bio-inspired or biodegradable porphyrins may provide new, cost-effective solutions compatible with scalable hydrogen production. Finally, alternative sacrificial agents that are both effective and less toxic should be explored to further enhance sustainability in photocatalytic hydrogen production.

Author Contributions: Writing—original draft preparation: D.R.B.; original draft preparation, writing: A.S.; original draft preparation, writing: E.O.; writing—review and editing: A.G.C.; writing—review and editing: R.I.K.; writing—review and editing: A.C.M.; visualization, supervision, original draft preparation, writing: K.L. All authors have read and agreed to the published version of the manuscript.

Funding: This research received no external funding.

Institutional Review Board Statement: Not applicable.

Informed Consent Statement: Not applicable.

Data Availability Statement: No new data were created or analyzed in this study.

Conflicts of Interest: The authors declare no conflicts of interest.

References

1. Lewis, N.S.; Nocera, D.G. Powering the planet: Chemical challenges in solar energy utilization. *Proc. Natl. Acad. Sci. USA* **2006**, *103*, 15729–15735. [CrossRef] [PubMed]
2. Global Energy Crisis. Available online: https://www.iea.org/topics/global-energy-crisis (accessed on 14 January 2025).
3. Zayer Kabeh, K.; Teimouri, A.; Changizian, S.; Ahmadi, P. Techno-economic assessment of small-scale gas to liquid technology to reduce waste flare gas in a refinery plant. *Sustain. Energy Technol. Assess.* **2023**, *55*, 102955. [CrossRef]
4. Yue, M.; Lambert, H.; Pahon, E.; Roche, R.; Jemei, S.; Hissel, D. Hydrogen energy systems: A critical review of technologies, applications, trends and challenges. *Renew. Sustain. Energy Rev.* **2021**, *146*, 111180. [CrossRef]
5. Teets, T.S.; Nocera, D.G. Photocatalytic hydrogen production. *Chem. Commun.* **2011**, *47*, 9268–9274. [CrossRef]
6. Van Hoecke, L.; Laffineur, L.; Campe, R.; Perreault, P.; Verbruggen, S.W.; Lenaerts, S. Challenges in the use of hydrogen for maritime applications. *Energy Environ. Sci.* **2021**, *14*, 815–843. [CrossRef]
7. Wei, D.; Shi, X.; Qu, R.; Junge, K.; Junge, H.; Beller, M. Toward a Hydrogen Economy: Development of Heterogeneous Catalysts for Chemical Hydrogen Storage and Release Reactions. *ACS Energy Lett.* **2022**, *7*, 3734–3752. [CrossRef]
8. Love, J.G.; O'Mullane, A.P.; Boulaire, F.A.; Mackinnon, I.D.R. Impact of fuel cells on hydrogen energy pathways in a sustainable energy economy. *Sustain. Energy Fuels* **2022**, *6*, 4008–4023. [CrossRef]

9. van der Spek, M.; Banet, C.; Bauer, C.; Gabrielli, P.; Goldthorpe, W.; Mazzotti, M.; Munkejord, S.T.; Røkke, N.A.; Shah, N.; Sunny, N.; et al. Perspective on the hydrogen economy as a pathway to reach net-zero CO_2 emissions in Europe. *Energy Environ. Sci.* **2022**, *15*, 1034–1077. [CrossRef]
10. Park, H.; Park, Y.; Kim, W.; Choi, W. Surface modification of TiO_2 photocatalyst for environmental applications. *J. Photochem. Photobiol. C Photochem. Rev.* **2013**, *15*, 1–20. [CrossRef]
11. Orfanos, E.; Ladomenou, K.; Angaridis, P.A.; Papadopoulos, T.; Charalambidis, G.; Vasilopoulou, M.; Coutsolelos, A.G. A stable platinum porphyrin based photocatalyst for hydrogen production under visible light in water. *Sustain. Energy Fuels* **2022**, *6*, 5072–5076. [CrossRef]
12. You, B.; Sun, Y. Innovative Strategies for Electrocatalytic Water Splitting. *Acc. Chem. Res.* **2018**, *51*, 1571–1580. [CrossRef] [PubMed]
13. Huang, L.-Y.; Huang, J.-F.; Lei, Y.; Qin, S.; Liu, J.-M. Porous Hybrid Materials Based on Mesotetrakis(Hydroxyphenyl) Porphyrins and TiO_2 for Efficient Visible-Light-Driven Hydrogen Production. *Catalysts* **2020**, *10*, 656. [CrossRef]
14. Ladomenou, K.; Natali, M.; Iengo, E.; Charalampidis, G.; Scandola, F.; Coutsolelos, A.G. Photochemical hydrogen generation with porphyrin-based systems. *Coord. Chem. Rev.* **2015**, *304–305*, 38–54. [CrossRef]
15. Hausmann, J.N.; Schlögl, R.; Menezes, P.W.; Driess, M. Is direct seawater splitting economically meaningful? *Energy Environ. Sci.* **2021**, *14*, 3679–3685. [CrossRef]
16. Yang, X.; Wang, D. Photocatalysis: From Fundamental Principles to Materials and Applications. *ACS Appl. Energy Mater.* **2018**, *1*, 6657–6693. [CrossRef]
17. Zhu, S.; Wang, D. Photocatalysis: Basic Principles, Diverse Forms of Implementations and Emerging Scientific Opportunities. *Adv. Energy Mater.* **2017**, *7*, 1700841. [CrossRef]
18. Checchetti, A.; Fantini, A. Experimental Determination of Planck's constant using Light Emitting Diodes (LEDs) and Photoelectric Effect. *World J. Chem. Educ.* **2015**, *3*, 87–92. [CrossRef]
19. Jaffe, H.H.; Miller, A.L. The fates of electronic excitation energy. *J. Chem. Educ.* **1966**, *43*, 469. [CrossRef]
20. Belver, C.; Bedia, J.; Gómez-Avilés, A.; Peñas-Garzón, M.; Rodriguez, J.J. Chapter 22—Semiconductor Photocatalysis for Water Purification. In *Nanoscale Materials in Water Purification*; Thomas, S., Pasquini, D., Leu, S.-Y., Gopakumar, D.A., Eds.; Elsevier: Amsterdam, The Netherlands, 2019; pp. 581–651. [CrossRef]
21. Li, S.; Xu, W.; Meng, L.; Tian, W.; Li, L. Recent Progress on Semiconductor Heterojunction-Based Photoanodes for Photoelectrochemical Water Splitting. *Small Sci.* **2022**, *2*, 2100112. [CrossRef]
22. Bahnemann, D.W.; Hilgendorff, M.; Memming, R. Charge Carrier Dynamics at TiO_2 Particles: Reactivity of Free and Trapped Holes. *J. Phys. Chem. B* **1997**, *101*, 4265–4275. [CrossRef]
23. Zhao, D.; Zhuang, Z.; Cao, X.; Zhang, C.; Peng, Q.; Chen, C.; Li, Y. Atomic site electrocatalysts for water splitting, oxygen reduction and selective oxidation. *Chem. Soc. Rev.* **2020**, *49*, 2215–2264. [CrossRef]
24. Goddard, W.A. Electrocatalytic Water Splitting ($H_2O \rightarrow H_2 + ½\ O_2$). In *Computational Materials, Chemistry, and Biochemistry: From Bold Initiatives to the Last Mile: In Honor of William A. Goddard's Contributions to Science and Engineering*; Shankar, S., Muller, R., Dunning, T., Chen, G.H., Eds.; Springer International Publishing: Cham, Switzerland, 2021; pp. 1257–1264. [CrossRef]
25. Zhang, W.L.; Wei, W.; Liu, W.; Guan, T.; Tian, Y.; Zeng, H. Engineering the morphology of TiO_2/carbon hybrids via oxidized Ti_3C_2Tx MXene and associated electrorheological activities. *Chem. Eng. J.* **2019**, *378*, 122170. [CrossRef]
26. Wang, H.-X.; Li, X.-X.; Tang, L. Effects of surfactants on the morphology and properties of TiO_2. *Appl. Phys. A* **2020**, *126*, 448. [CrossRef]
27. Najafi, M.; Kermanpur, A.; Rahimipour, M.R.; Najafizadeh, A. Effect of TiO_2 morphology on structure of TiO_2-graphene oxide nanocomposite synthesized via a one-step hydrothermal method. *J. Alloys Compd.* **2017**, *722*, 272–277. [CrossRef]
28. Nasir, J.A.; Rehman, Z.u.; Shah, S.N.A.; Khan, A.; Butler, I.S.; Catlow, C.R.A. Recent developments and perspectives in CdS-based photocatalysts for water splitting. *J. Mater. Chem. A* **2020**, *8*, 20752–20780. [CrossRef]
29. Zaleska, A. Doped-TiO_2: A Review. *Recent Pat. Eng.* **2008**, *2*, 157–164. [CrossRef]
30. Yang, D.-X.; Qu, D.; Miao, X.; Jiang, W.-S.; An, L.; Wen, Y.-J.; Wu, D.-D.; Sun, Z.-C. TiO_2 sensitized by red-, green-, blue-emissive carbon dots for enhanced H_2 production. *Rare Met.* **2019**, *38*, 404–412. [CrossRef]
31. Rajaambal, S.; Sivaranjani, K.; Gopinath, C.S. Recent developments in solar H_2 generation from water splitting. *J. Chem. Sci.* **2015**, *127*, 33–47. [CrossRef]
32. Ye, Z.; Kong, L.; Chen, F.; Chen, Z.; Lin, Y.; Liu, C. A comparative study of photocatalytic activity of ZnS photocatalyst for degradation of various dyes. *Optik* **2018**, *164*, 345–354. [CrossRef]
33. Ajibade, P.A.; Mbuyazi, T.B.; Oluwalana, A.E. Lead Sulphide Nanoparticles as Photocatalyst for the Degradation of Methylene Blue: Effects of pH, Time, Adsorption Kinetics and Recyclability Studies. *J. Inorg. Organomet. Polym. Mater.* **2021**, *31*, 2197–2208. [CrossRef]
34. Luttrell, T.; Halpegamage, S.; Tao, J.; Kramer, A.; Sutter, E.; Batzill, M. Why is anatase a better photocatalyst than rutile?—Model studies on epitaxial TiO_2 films. *Sci. Rep.* **2014**, *4*, 4043. [CrossRef] [PubMed]

35. Bourikas, K.; Kordulis, C.; Lycourghiotis, A. Titanium Dioxide (Anatase and Rutile): Surface Chemistry, Liquid–Solid Interface Chemistry, and Scientific Synthesis of Supported Catalysts. *Chem. Rev.* **2014**, *114*, 9754–9823. [CrossRef]
36. Khlyustova, A.; Sirotkin, N.; Kusova, T.; Kraev, A.; Titov, V.; Agafonov, A. Doped TiO_2: The effect of doping elements on photocatalytic activity. *Mater. Adv.* **2020**, *1*, 1193–1201. [CrossRef]
37. Sultana, M.; Mondal, A.; Islam, S.; Khatun, M.A.; Rahaman, M.H.; Chakraborty, A.K.; Rahman, M.S.; Rahman, M.M.; Nur, A.S.M. Strategic development of metal doped TiO_2 photocatalysts for enhanced dye degradation activity under UV–Vis irradiation: A review. *Curr. Res. Green Sustain. Chem.* **2023**, *7*, 100383. [CrossRef]
38. Cai, Y.; Feng, Y.P. Review on charge transfer and chemical activity of TiO_2: Mechanism and applications. *Prog. Surf. Sci.* **2016**, *91*, 183–202. [CrossRef]
39. Fujishima, A.; Honda, K. Electrochemical Photolysis of Water at a Semiconductor Electrode. *Nature* **1972**, *238*, 37–38. [CrossRef] [PubMed]
40. Bahnemann, D.; Henglein, A.; Lilie, J.; Spanhel, L. Flash photolysis observation of the absorption spectra of trapped positive holes and electrons in colloidal titanium dioxide. *J. Phys. Chem.* **1984**, *88*, 709–711. [CrossRef]
41. Xu, Y.; Qiu, F.; Xu, S.-Q.; Zhu, S.; Zhang, Y.; Liu, H.; Zong, P.; Ma, L.; Hong, K.; Wang, Y. Boosting Photocatalytic Hydrogen Evolution by a Light Coupling and Charge Carrier Confinement Strategy. *Adv. Funct. Mater.* **2025**, *35*, 2417553. [CrossRef]
42. Gao, W.; Lu, J.; Zhang, S.; Zhang, X.; Wang, Z.; Qin, W.; Wang, J.; Zhou, W.; Liu, H.; Sang, Y. Suppressing Photoinduced Charge Recombination via the Lorentz Force in a Photocatalytic System. *Adv. Sci.* **2019**, *6*, 1901244. [CrossRef]
43. Guo, Q.; Zhou, C.; Ma, Z.; Yang, X. Fundamentals of TiO_2 Photocatalysis: Concepts, Mechanisms, and Challenges. *Adv. Mater.* **2019**, *31*, 1901997. [CrossRef]
44. Rahimi, N.; Pax, R.A.; Gray, E.M. Review of functional titanium oxides. I: TiO_2 and its modifications. *Prog. Solid State Chem.* **2016**, *44*, 86–105. [CrossRef]
45. Humayun, M.; Raziq, F.; Khan, A.; Luo, W. Modification strategies of TiO_2 for potential applications in photocatalysis: A critical review. *Green Chem. Lett. Rev.* **2018**, *11*, 86–102. [CrossRef]
46. Augustin, A.; Ganguly, P.; Shenoy, S.; Chuaicham, C.; Pillai, S.C.; Sasaki, K.; Lee, A.F.; Sekar, K. Impact of Hole Scavengers on Efficient Photocatalytic Hydrogen Production. *Adv. Sustain. Syst.* **2024**, *8*, 2400321. [CrossRef]
47. Rozman, N.; Nadrah, P.; Cornut, R.; Jousselme, B.; Bele, M.; Dražić, G.; Gaberšček, M.; Kunej, Š.; Škapin, A.S. TiO_2 photocatalyst with single and dual noble metal co-catalysts for efficient water splitting and organic compound removal. *Int. J. Hydrogen Energy* **2021**, *46*, 32871–32881. [CrossRef]
48. Ding, D.; Liu, K.; He, S.; Gao, C.; Yin, Y. Ligand-Exchange Assisted Formation of Au/TiO_2 Schottky Contact for Visible-Light Photocatalysis. *Nano Lett.* **2014**, *14*, 6731–6736. [CrossRef]
49. Yu, S.; Han, B.; Lou, Y.; Liu, Z.; Qian, G.; Wang, Z. Rational design and fabrication of TiO_2 nano heterostructure with multi-junctions for efficient photocatalysis. *Int. J. Hydrogen Energy* **2020**, *45*, 28640–28650. [CrossRef]
50. Brady, M.D.; Sampaio, R.N.; Wang, D.; Meyer, T.J.; Meyer, G.J. Dye-Sensitized Hydrobromic Acid Splitting for Hydrogen Solar Fuel Production. *J. Am. Chem. Soc.* **2017**, *139*, 15612–15615. [CrossRef]
51. Jaafar, S.N.H.; Minggu, L.J.; Arifin, K.; Kassim, M.B.; Wan, W.R.D. Natural dyes as TIO_2 sensitizers with membranes for photoelectrochemical water splitting: An overview. *Renew. Sustain. Energy Rev.* **2017**, *78*, 698–709. [CrossRef]
52. Nikolaou, V.; Charalambidis, G.; Ladomenou, K.; Nikoloudakis, E.; Drivas, C.; Vamvasakis, I.; Panagiotakis, S.; Landrou, G.; Agapaki, E.; Stangel, C.; et al. Controlling Solar Hydrogen Production by Organizing Porphyrins. *ChemSusChem* **2021**, *14*, 961–970. [CrossRef]
53. Mulewa, W.; Tahir, M.; Amin, N.A.S. MMT-supported Ni/TiO_2 nanocomposite for low temperature ethanol steam reforming toward hydrogen production. *Chem. Eng. J.* **2017**, *326*, 956–969. [CrossRef]
54. Xing, X.; Zhang, M.; Hou, L.; Xiao, L.; Li, Q.; Yang, J. Z-scheme BCN-TiO_2 nanocomposites with oxygen vacancy for high efficiency visible light driven hydrogen production. *Int. J. Hydrogen Energy* **2017**, *42*, 28434–28444. [CrossRef]
55. Muñoz-Batista, M.J.; Rodríguez-Padrón, D.; Puente-Santiago, A.R.; Kubacka, A.; Luque, R.; Fernández-García, M. Sunlight-Driven Hydrogen Production Using an Annular Flow Photoreactor and g-C3N4-Based Catalysts. *ChemPhotoChem* **2018**, *2*, 870–877. [CrossRef]
56. Sun, S. N-Doped TiO_2 Nanobelts with Coexposed (001) and (101) Facets and Their Highly Efficient Visible-Light-Driven Photocatalytic Hydrogen Production. *ACS Appl. Mater.* **2016**, *8*, 18126–18131. [CrossRef]
57. Wu, M.-C.; Hiltunen, J.; Sápi, A.; Avila, A.; Larsson, W.; Liao, H.-C.; Huuhtanen, M.; Tóth, G.; Shchukarev, A.; Laufer, N.; et al. Nitrogen-Doped Anatase Nanofibers Decorated with Noble Metal Nanoparticles for Photocatalytic Production of Hydrogen. *ACS Nano* **2011**, *5*, 5025–5030. [CrossRef]
58. Kumaravel, V.; Mathew, S.; Bartlett, J.; Pillai, S.C. Photocatalytic hydrogen production using metal doped TiO_2: A review of recent advances. *Appl. Catal. B Environ.* **2019**, *244*, 1021–1064. [CrossRef]
59. Banerjee, B.; Amoli, V.; Maurya, A.; Sinha, A.K.; Bhaumik, A. Green synthesis of Pt-doped TiO_2 nanocrystals with exposed (001) facets and mesoscopic void space for photo-splitting of water under solar irradiation. *Nanoscale* **2015**, *7*, 10504–10512. [CrossRef]

60. Fontelles-Carceller, O.; Muñoz-Batista, M.J.; Rodríguez-Castellón, E.; Conesa, J.C.; Fernández-García, M.; Kubacka, A. Measuring and interpreting quantum efficiency for hydrogen photo-production using Pt-titania catalysts. *J. Catal.* **2017**, *347*, 157–169. [CrossRef]
61. Fang, J.; Cao, S.-W.; Wang, Z.; Shahjamali, M.M.; Loo, S.C.J.; Barber, J.; Xue, C. Mesoporous plasmonic Au–TiO_2 nanocomposites for efficient visible-light-driven photocatalytic water reduction. *Int. J. Hydrogen Energy* **2012**, *37*, 17853–17861. [CrossRef]
62. Gogoi, D.; Namdeo, A.; Golder, A.K.; Peela, N.R. Ag-doped TiO_2 photocatalysts with effective charge transfer for highly efficient hydrogen production through water splitting. *Int. J. Hydrogen Energy* **2020**, *45*, 2729–2744. [CrossRef]
63. Ouyang, W.; Muñoz-Batista, M.J.; Kubacka, A.; Luque, R.; Fernández-García, M. Enhancing photocatalytic performance of TiO_2 in H_2 evolution via Ru co-catalyst deposition. *Appl. Catal. B Environ.* **2018**, *238*, 434–443. [CrossRef]
64. Díaz, L.; Rodríguez, V.D.; González-Rodríguez, M.; Rodríguez-Castellón, E.; Algarra, M.; Núñez, P.; Moretti, E. M/TiO_2 (M = Fe, Co, Ni, Cu, Zn) catalysts for photocatalytic hydrogen production under UV and visible light irradiation. *Inorg. Chem. Front.* **2021**, *8*, 3491–3500. [CrossRef]
65. David, T.M.; Dev, P.R.; Wilson, P.; Sagayaraj, P.; Mathews, T. A critical review on the variations in anodization parameters toward microstructural formation of TiO_2 nanotubes. *Electrochem. Sci. Adv.* **2022**, *2*, e202100083. [CrossRef]
66. Sadanandam, G.; Lalitha, K.; Kumari, V.D.; Shankar, M.V.; Subrahmanyam, M. Cobalt doped TiO_2: A stable and efficient photocatalyst for continuous hydrogen production from glycerol: Water mixtures under solar light irradiation. *Int. J. Hydrogen Energy* **2013**, *38*, 9655–9664. [CrossRef]
67. Dholam, R.; Patel, N.; Adami, M.; Miotello, A. Hydrogen production by photocatalytic water-splitting using Cr- or Fe-doped TiO_2 composite thin films photocatalyst. *Int. J. Hydrogen Energy* **2009**, *34*, 5337–5346. [CrossRef]
68. Tudu, B.; Nalajala, N.; Prabhakar Reddy, K.; Saikia, P.; Gopinath, C.S. Rationally Designed, Efficient, and Earth-Abundant Ni–Fe Cocatalysts for Solar Hydrogen Generation. *ACS Sustain. Chem. Eng.* **2021**, *9*, 13915–13925. [CrossRef]
69. Pinna, M.; Wei, A.W.W.; Spanu, D.; Will, J.; Yokosawa, T.; Spiecker, E.; Recchia, S.; Schmuki, P.; Altomare, M. Amorphous NiCu Thin Films Sputtered on TiO_2 Nanotube Arrays: A Noble-Metal Free Photocatalyst for Hydrogen Evolution. *ChemCatChem* **2022**, *14*, e202201052. [CrossRef]
70. Gao, D.; Liu, W.; Xu, Y.; Wang, P.; Fan, J.; Yu, H. Core-shell Ag@Ni cocatalyst on the TiO_2 photocatalyst: One-step photoinduced deposition and its improved H_2-evolution activity. *Appl. Catal. B Environ.* **2020**, *260*, 118190. [CrossRef]
71. Ngo, N.M.; Nguyen, M.D.; Tran, H.-V.; Medhi, R.; Lee, J.M.; Lee, T.R. Photocatalytic Hydrogen Generation by Monodisperse TiO_2 Nanoparticles Singly and Dually Doped with Niobium and Tantalum. *ACS Appl. Nano Mater.* **2025**, *8*, 4841–4851. [CrossRef]
72. Afrin, M.F.; Furukawa, M.; Tateishi, I.; Katsumata, H.; Uzzaman, M.; Kaneco, S. Enhanced Photocatalytic Hydrogen Generation from Methanol Solutions via In Situ Ni/Pt Co-Deposition on TiO_2. *J. Compos. Sci.* **2025**, *9*, 68. [CrossRef]
73. Ibrahim, N.S.; Leaw, W.L.; Mohamad, D.; Alias, S.H.; Nur, H. A critical review of metal-doped TiO_2 and its structure–physical properties–photocatalytic activity relationship in hydrogen production. *Int. J. Hydrogen Energy* **2020**, *45*, 28553–28565. [CrossRef]
74. Charisiadis, A.; Nikolaou, V.; Nikoloudakis, E.; Ladomenou, K.; Charalambidis, G.; Coutsolelos, A.G. Metalloporphyrins in bio-inspired photocatalytic conversions. *Chem. Commun.* **2025**, *61*, 4630–4646. [CrossRef]
75. Landrou, G.; Panagiotopoulos, A.A.; Ladomenou, K.; Coutsolelos, A.G. Photochemical hydrogen evolution using Sn-porphyrin as photosensitizer and a series of Cobaloximes as catalysts. *J. Porphyr. Phthalocyanines* **2016**, *20*, 534–541. [CrossRef]
76. Xing, X.; Zhu, H.; Zhang, M.; Hou, L.; Li, Q.; Yang, J. Interfacial oxygen vacancy layer of a Z-scheme BCN–TiO_2 heterostructure accelerating charge carrier transfer for visible light photocatalytic H_2 evolution. *Catal. Sci. Technol.* **2018**, *8*, 3629–3637. [CrossRef]
77. Guo, X.; Li, X.; Qin, L.; Kang, S.-Z.; Li, G. A highly active nano-micro hybrid derived from Cu-bridged TiO_2/porphyrin for enhanced photocatalytic hydrogen production. *Appl. Catal. B Environ.* **2019**, *243*, 1–9. [CrossRef]
78. Gonuguntla, S.; Tiwari, A.; Madanaboina, S.; Lingamallu, G.; Pal, U. Revealing high hydrogen evolution activity in zinc porphyrin sensitized hierarchical porous TiO_2 photocatalysts. *Int. J. Hydrogen Energy* **2020**, *45*, 7508–7516. [CrossRef]
79. Chanda, N.; Koteshwar, D.; Gonuguntla, S.; Bojja, S.; Pal, U.; Giribabu, L. Efficient visible-light-driven hydrogen production by Zn–porphyrin based photocatalyst with engineered active donor–acceptor sites. *Mater. Adv.* **2021**, *2*, 4762–4771. [CrossRef]
80. Gkika, D.A.; Ladomenou, K.; Bououdina, M.; Mitropoulos, A.C.; Kyzas, G.Z. Adsorption and photocatalytic applications of porphyrin-based materials for environmental separation processes: A review. *Sci. Total Environ.* **2024**, *908*, 168293. [CrossRef]
81. Nikoloudakis, E.; López-Duarte, I.; Charalambidis, G.; Ladomenou, K.; Ince, M.; Coutsolelos, A.G. Porphyrins and phthalocyanines as biomimetic tools for photocatalytic H_2 production and CO_2 reduction. *Chem. Soc. Rev.* **2022**, *51*, 6965–7045. [CrossRef]
82. Nikolaou, V.; Agapaki, E.; Nikoloudakis, E.; Achilleos, K.; Ladomenou, K.; Charalambidis, G.; Triantafyllou, E.; Coutsolelos, A.G. Highly efficient light-driven hydrogen evolution utilizing porphyrin-based nanoparticles. *Chem. Commun.* **2023**, *59*, 11256–11259. [CrossRef]
83. Agapaki, E.; Ladomenou, K.; Nikolaou, V.; Coutsolelos, A.G. Efficient solar hydrogen production of zinc trimesityl porphyrin-based photocatalysts. *J. Porphyr. Phthalocyanines* **2023**, *27*, 479–489. [CrossRef]

84. Wang, D.; Niu, L.; Qiao, Z.-Y.; Cheng, D.-B.; Wang, J.; Zhong, Y.; Bai, F.; Wang, H.; Fan, H. Synthesis of Self-Assembled Porphyrin Nanoparticle Photosensitizers. *ACS Nano* **2018**, *12*, 3796–3803. [CrossRef] [PubMed]
85. Wang, Q.; Shi, Y.; Ma, Q.; Gao, D.; Zhong, J.; Li, J.; Wang, F.; He, Y.; Wang, R. A flower-like TiO_2 with photocatalytic hydrogen evolution activity modified by Zn(II) porphyrin photocatalysts. *J. Mater. Sci. Mater. Electron.* **2017**, *28*, 2123–2127. [CrossRef]
86. Zhu, H.; Zhu, W.; Kang, S.-Z.; Qin, L.; Zhang, T.; Li, X. Facile interfacial modification in a novel TiO_2/porphyrin nano-micro hybrid for dual functions of boosting photocatalytic H_2 production and methylene blue degradation. *Appl. Surf. Sci.* **2024**, *644*, 158783. [CrossRef]
87. Liu, Y.; Lv, X.; Zhong, Y.; Wang, G.; Liu, S.; Chen, S.; Qi, C.; He, M.; Shangguan, P.; Luo, Z.; et al. Self-Assembly Regulated Photocatalysis of Porphyrin-TiO_2 Nanocomposites. *Molecules* **2024**, *29*, 3872. [CrossRef]
88. Wang, S.; Hu, G.; Dou, Y.; Li, S.; Li, M.; Feng, H.; Feng, Y.-S. Z-scheme promoted interfacial charge transfer on Cu/In-porphyrin MOFs/CdIn2S4 heterostructure for efficient photocatalytic H_2 evolution. *Sep. Purif. Technol.* **2025**, *354*, 129220. [CrossRef]
89. Myltykbayeva, Z.; López Nieto, J.M.; Moreno-Torralbo, B.M.; Concepción, P.; Abylaikhan, A.; Koca, A. Optimizing the electrocatalytic hydrogen production with vanadyl porphyrin impregnated on mesoporous SiO_2 nanoparticles. *Electrochim. Acta* **2025**, *514*, 145686. [CrossRef]
90. Xiao, L.; Zhang, Q.; Wang, X.; Li, B.; Li, X.; Yang, X.; Li, W.; Zhang, H. Integration of platinum nanoparticles and Pd-porphyrin photosensitiser into a metal–organic framework for effective photocatalytic hydrogen evolution. *J. Colloid Interface Sci.* **2025**, *685*, 165–172. [CrossRef]
91. Van Tran, C.; Dang, T.-D.; Lai, V.D.; Thi Nguyen, G.; Thi Hoa, B.; Nguyen, H.T.; Thi, H.P.N.; Nguyen, T.T.; La, D.D. Self-assembly of porphyrin nanofiber on the surface $CuFe_2O_4$ nanoparticles: A novel photoanode for enhanced photo-electrochemical water splitting. *Fuel* **2025**, *380*, 133196. [CrossRef]

Disclaimer/Publisher's Note: The statements, opinions and data contained in all publications are solely those of the individual author(s) and contributor(s) and not of MDPI and/or the editor(s). MDPI and/or the editor(s) disclaim responsibility for any injury to people or property resulting from any ideas, methods, instructions or products referred to in the content.